Climatic Change
DOI 10.1007/s10584-010-9847-0

Precipitation extremes and the impacts of climate change on stormwater infrastructure in Washington State

Eric A. Rosenberg · Patrick W. Keys · Derek B. Booth · David Hartley · Jeff Burkey · Anne C. Steinemann · Dennis P. Lettenmaier

Received: 4 June 2009 / Accepted: 23 March 2010

Abstract The design of stormwater infrastructure is based on an underlying assumption that the probability distribution of precipitation extremes is statistically stationary. This assumption is called into question by climate change, resulting in uncertainty about the future performance of systems constructed under this paradigm. We therefore examined both historical precipitation records and simulations of future rainfall to evaluate past and prospective changes in the probability distributions of precipitation extremes across Washington State. Our historical analyses were based on hourly precipitation records for the time period 1949–2007 from weather stations in and near the state's three major metropolitan areas: the Puget Sound region, Vancouver (WA), and Spokane. Changes in future precipitation were evaluated using two runs of the Weather Research and Forecast (WRF) regional climate model (RCM) for the time periods 1970–2000 and 2020–2050, dynamically downscaled from the ECHAM5 and CCSM3 global climate models. Bias-corrected and statistically downscaled hourly precipitation sequences were then used as input

E. A. Rosenberg (✉) · P. W. Keys · D. B. Booth · A. C. Steinemann · D. P. Lettenmaier
Department of Civil and Environmental Engineering, University of Washington,
Box 352700, Seattle, WA 98195–2700, USA
e-mail: ericrose@u.washington.edu

D. B. Booth
Stillwater Sciences, P.O. Box 904, Santa Barbara, CA 93102, USA

D. Hartley
Northwest Hydraulic Consultants, 16300 Christensen Road,
Suite 350, Seattle, WA 98188-3422, USA

J. Burkey
King County Water and Land Resources Division,
516 Third Avenue, Seattle, WA 98104, USA

A. C. Steinemann
Evans School of Public Affairs, University of Washington,
Box 353055, Seattle, WA 98195-3055, USA

Published online: 22 April 2010

to the HSPF hydrologic model to simulate streamflow in two urban watersheds in central Puget Sound. Few statistically significant changes were observed in the historical records, with the possible exception of the Puget Sound region. Although RCM simulations generally predict increases in extreme rainfall magnitudes, the range of these projections is too large at present to provide a basis for engineering design, and can only be narrowed through consideration of a larger sample of simulated climate data. Nonetheless, the evidence suggests that drainage infrastructure designed using mid-20th century rainfall records may be subject to a future rainfall regime that differs from current design standards.

1 Introduction

Infrastructure is commonly defined as the various components of the built environment that support modern society (e.g., Choguill 1996; Hanson 1984). These encompass utilities, transportation systems, communication networks, water systems, and other elements that include some of the most critical underpinnings of civilization. Thus even modest disruptions to infrastructure can have significant effects on daily life, and any systematic change in the frequency or intensity of those disruptions could have profound consequences for economic and human well-being.

The daily news provides frequent examples of those elements of our infrastructure that are most vulnerable to the vagaries of even present-day fluctuations in weather. The Chehalis River floods in December 2007, for example, resulted in the closure of Interstate 5, Washington State's major north–south transportation artery, for four days at an estimated cost of over $18 M (WSDOT 2008). The various elements of Washington's infrastructure are not equally vulnerable to weather conditions or climate regimes, however, and several of these elements (specifically energy and water supply facilities) are the subject of other papers in this issue (Hamlet et al. 2010; Vano et al. 2010a, b). The overarching scope for this paper was to characterize the potential impacts of climate change on stormwater infrastructure systems.

To understand the impacts that could occur, we first reviewed the literature and prior work, and conducted interviews with state and local public works officials who deal with the consequences of inadequate stormwater infrastructure on a daily basis. Although many types of climate-related impacts to infrastructure are possible, this reconnaissance clearly indicated that stormwater impacts of a changing climate are a major concern but are not well understood. The Intergovernmental Panel on Climate Change (IPCC) cites a 90% chance of increased frequency of heavy rainfall events in the 21st century and a potential increase in higher-latitude stormwater runoff by as much as 10–40% (IPCC 2007a), changes that would have obvious repercussions on stormwater management. Recent improvements in the ability to downscale the projections of global climate models to the local scale (Salathé 2005) now make feasible the preliminary evaluation of climate change impacts on the spatially heterogeneous, rapidly fluctuating behavior of urban stormwater. This evaluation is warranted, because although the consequences of inadequate stormwater facilities can be severe, adaptation strategies are available and relatively straightforward if anticipated well in advance (Kirschen et al. 2004; Larsen and Goldsmith 2007; Shaw et al. 2005).

Historical management goals for urban stormwater have emphasized safe conveyance, with more recent attention also being given to the consequences of

increased streamflows on the physical and biological integrity of downstream channels (Booth and Jackson 1997). Urbonas and Roesner (1993) classify drainage systems into two categories: minor, consisting of roadside swales, gutters, and sewers that are typically designed to convey runoff events of 2- to 5-year return periods; and major, which include the larger flood control structures designed to manage 50- to 100-year events. While design events can be based on direct observations of runoff, they are more commonly based on precipitation events with equivalent likelihoods of occurrence, due to the limited availability of runoff measurements in urban areas. Hence, while we give some consideration to modeled trends in runoff, the focus of this paper is mostly on the precipitation events from which they result, and specifically those events of 1-h duration (since many of the smaller watersheds have times of concentration of 1 h or less) and 24-h duration (which is often used for the design of larger structures).

It is worth noting that more hydrologically complicated phenomena with implications for stormwater management, such as rain-on-snow events, are also subject to the effects of a changing climate. We do not consider trends in these phenomena, which are relatively unimportant in the lowland urban areas that are the focus of our study. Nor do we consider changing patterns of development, which may also considerably impact runoff magnitudes but are not related to climatic factors. Nonetheless, future changes in climate that may alter precipitation intensity or duration would likely have consequences for urban stormwater discharge, particularly where stormwater detention and conveyance facilities were designed under assumptions that may no longer be correct. While we recognize the social and economic impacts of increasing the capacity of undersized stormwater facilities, or the disabling of key assets because of more severe flooding, these considerations are beyond the scope of the present study.

This paper addresses the following questions:

- What are the historical trends in precipitation extremes across Washington State?
- What are the projected trends in precipitation extremes over the next 50 years in the state's urban areas?
- What are the likely consequences of future changes in precipitation extremes on urban stormwater infrastructure?

2 Background

Despite the inherent challenges in characterizing changes in extreme rainfall events, a number of studies have either assessed historical trends in precipitation metrics or investigated the vulnerability of stormwater infrastructure under a changing climate. We briefly summarize a few key studies that are most relevant to our work below.

2.1 Historical trends in precipitation extremes

Several studies have evaluated past trends in rainfall extremes of various durations, mostly at national or global scales. Karl and Knight (1998) found a 10% increase in total annual precipitation across the contiguous USA since 1910, and attributed over half of the increase to positive trends in both frequency and intensity in the

upper ten percent of the daily precipitation distribution. Kunkel et al. (1999) found a national increase of 16% from 1931–1996 in the frequency of 7-day extreme precipitation events, although no statistically significant trend was found for the Pacific Northwest. A follow-up study that employed data extending to 1895 (Kunkel et al. 2003) generally reinforced these findings but noted that frequencies for some return periods were nearly as high at the beginning of the 20th century as they were at the end, suggesting that natural variability could not be discounted as an important contributor to the observed trends.

Groisman et al. (2005) analyzed precipitation data over half of the global land area and found "an increasing probability of intense precipitation events for many extratropical regions including the US." They defined intense precipitation events as the upper 0.3% of daily observations and used three model simulations with transient greenhouse gas increases to offer preliminary evidence that these trends are linked to global warming. Pryor et al. (2009) analyzed eight metrics of precipitation in century-long records throughout the contiguous USA and found that statistically significant trends generally indicated increases in intensity of events above the 95th percentile, although few of these were located in Washington State. Madsen and Figdor (2007), in a study that systematically analyzed trends from 1948 to 2006 by both state and metropolitan area, found statistically significant increases of 30% in the frequency of extreme precipitation in Washington and 45% in the Seattle–Tacoma–Bremerton area. Interestingly, however, trends in neighboring states were widely incongruent, with a statistically significant decrease of 14% in Oregon and a non-significant increase of 1% in Idaho.

While these studies provide useful impressions of general trends in precipitation extremes, their results are not applicable to infrastructure design, which requires estimates of the distributions of extreme magnitudes instead of, for example, the number of exceedances of a fixed threshold. Relatively few such approaches have been explored to date, with the exception of Fowler and Kilsby (2003), who used regional frequency analysis to determine changes in design storms of 1-, 2-, 5-, and 10-day durations from 1961 to 2000 in the UK. We take their approach one step further and analyze changes in design storms of sub-daily durations, as discussed in Section 3.

2.2 Future projections and adaptation options

As noted above, few previous studies have evaluated the vulnerability of stormwater infrastructure to climate change, and those studies that have been performed vary considerably in their methodologies. Denault et al. (2002) assessed urban drainage capacity under future precipitation for a 440-ha (1080-ac) urban watershed in North Vancouver, Canada. Observed trends of precipitation intensity and magnitude for the period 1964–1997 were projected statistically to infer the magnitude of design storms in 2020 and 2050, and the consequences for urban discharges were modeled using the SWMM hydrologic model (http://www.epa.gov/ednnrmrl/models/swmm). The authors evaluated only the potential impacts on pipe capacity, finding that flow increases were sufficiently small that few infrastructure changes would be required. They also observed that any given watershed has unique characteristics that affect its ability to accommodate specific impacts, thus emphasizing the importance of site-specific evaluation.

Waters et al. (2003) evaluated how a small (23-ha [58-ac]) urban watershed in the Great Lakes region would be affected by a 15% increase in rainfall depth and intensity. This increase was prescribed based on a literature review and prior analysis of other nearby catchments. Their study emphasized the efficacy of adaptive measures that could absorb the increased rainfall, which they evaluated using SWMM. Recommended measures included downspout disconnection (50% of connected roofs), increased depression storage (by 45 m^3/impervious hectare [640 ft^3/impervious acre]), and increased street detention storage (by 40 m^3/impervious hectare [560 ft^3/impervious acre]).

Shaw et al. (2005) also studied the consequences of precipitation increases on stormwater systems, while relying on relatively simplistic projections of future precipitation. They defined low, medium and high climate-change scenarios based on projections of temperature increases, and translated those changes into linear increases in 24-h rainfall events. Using both event-based and continuous hydrologic models, consequences of inadequate capacity were then evaluated for stormwater systems in a small urban watershed of central New Zealand.

Watt et al. (2003) examined the multiple impacts that climate change could have on stormwater design and infrastructure in Canada, suggesting adaptive measures for urban watersheds and their associated advantages, disadvantages, and estimated costs. They also examined two case studies of adapting stormwater infrastructure to climate change—Waters et al. (2003) and a study of a residential area in urban Ottawa. They offered a qualitative rating system to compare the environmental, social, and aesthetic implications of different structural solutions to stormwater runoff management.

These prior studies provide a good methodological starting point for identifying the most likely consequences of climate change on stormwater infrastructure, along with an initial list of potentially useful adaptation measures. Like the approaches summarized in Section 2.1, however, their greatest collective shortcoming lies in their rudimentary characterization of the precipitation regimes that drive the responses (see also Kirschen et al. 2004; Trenberth et al. 2003). We seek to bridge this gap between prescribed (but poorly quantified) future climate change and the acknowledgment that infrastructure adaptation is generally less costly and disruptive if necessary measures are undertaken well in advance of anticipated changes.

We approach this task both by analyzing the variability in historical precipitation extremes across Washington State and by utilizing regional climate model (RCM) results, now available at a relatively high spatial resolution, to characterize future projections of precipitation extremes. We also apply a bias-correction and statistical-downscaling procedure to the RCM results to produce input precipitation series for a time-continuous hydrologic model, which in turn is used to predict streamflows in an urban lowland catchment in the Puget Sound region. These results facilitate a preliminary evaluation of the implications of simulated precipitation extremes for urban drainage and urban flooding.

3 Historical precipitation analysis

As a precursor to investigating potential changes in future precipitation extremes, we examined the extent to which trends in precipitation may have occurred in the three major urban areas of Washington State over the last half century. Three different

trend analysis methods were applied to historical rainfall records, beginning in 1949: (1) regional frequency analysis, (2) precipitation event analysis, and (3) exceedance-over-threshold analysis. In the regional frequency analysis, we used a technique adapted from the regional L-moments method of Hosking and Wallis (1997) as applied by Fowler and Kilsby (2003) to evaluate changes in rainfall extremes over the period 1956–2005 for a range of frequencies and durations. The precipitation event analysis used a method adapted from Karl and Knight (1998) to determine trends in annual precipitation event frequency and intensity, based on the occurrence of individual rainfall "events" of presumed one-day duration. Finally, the exceedance-over-threshold analysis examined the number of exceedances above a range of threshold values for the depth of precipitation, also on the basis of one-day rainfall events.

3.1 Regional frequency analysis

The precipitation frequency analysis analyzed the annual maximum series for aggregates of hourly precipitation ranging from 1 h to 10 days for the three major urban areas in Washington State: the Puget Sound region (including Seattle, Tacoma, and Olympia), the Vancouver, WA–Portland, OR region, and the Spokane region. Sometimes referred to as the index-flood approach, the technique entails fitting a frequency distribution to normalized annual maxima from a set of multiple stations rather than a single station, the premise being that all sites within a region can be described by a common probability distribution after site data are divided by their at-site means. These common probability distributions are referred to as regional growth curves. Design storms at individual sites can then be calculated by reversing the process and multiplying the regional growth curves by the at-site means. The strength of the method is in the regionalization, which provides a larger sampling pool and a more robust fit to the probability distribution, resulting in estimates of extreme quantiles that are considerably less variable than at-site estimates (see, e.g., Lettenmaier et al. 1987).

Data originated from National Climatic Data Center (NCDC) hourly precipitation archives and were extracted using commercial software provided by Earth Info, Inc. Stations selected for the analysis are shown in Fig. 1 and are listed in Table 1, with a minimum requirement of 40 years of record. Years with more than 10% missing data in the fall and winter months were removed from the analysis, since precipitation events during these two seasons contribute most of the annual maxima. Although many of the stations used gauges whose precision changed from 0.254 mm (0.01 in.) to 2.54 mm (0.1 in.) over the course of their records, this issue is somewhat minor for our analysis of annual maxima, which are substantially greater than a tenth of an inch at even the 1-h duration. Nonetheless, we evaluated the effect of these changes by repeating the analysis that follows on data rounded to the nearest tenth of an inch. None of the results differed significantly, however, and are thus not reported here.

The first step in the procedure was to identify annual maximum precipitation depths at multiple durations (1, 2, 3, 6, 12, and 24 h; and 2, 5, and 10 days), which were then combined into pools in order to calculate regional L-moment parameters (Fowler and Kilsby 2003; Hosking and Wallis 1997; Wallis et al. 2007). These parameters were used to fit data to Generalized Extreme Value (GEV) distributions and to generate regional growth curves. We then analyzed for any historical trends in

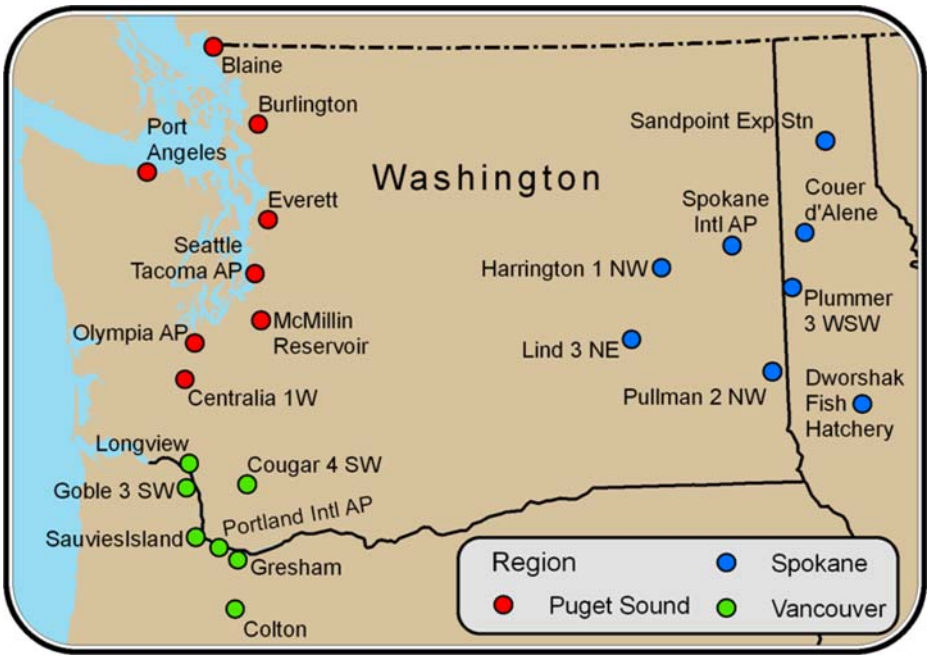

Fig. 1 Locations of weather stations used in the regional frequency analysis, grouped by region. Figure: Robert Norheim

Table 1 Stations used in the regional frequency analysis

Region	Station	State	Co-op ID	Reported period	No. of years removed	Sample size
Puget Sound	Blaine	WA	450729	1949–2007	14	45
	Burlington	WA	450986	1949–2007	21	38
	Centralia 1 W	WA	451277	1968–2007	18	22
	Everett	WA	452675	1949–2007	23	36
	McMillin Reservoir	WA	455224	1949–2007	25	34
	Olympia AP	WA	456114	1949–2007	8	51
	Port Angeles	WA	456624	1949–2007	25	34
	Seattle–Tacoma AP	WA	457473	1949–2007	0	59
Spokane	Couer d'Alene	ID	101956	1949–2007	33	26
	Dworshak Fish Hatchery	ID	102845	1967–2007	16	25
	Harrington 1 NW	WA	453515	1962–2007	19	27
	Lind 3 NE	WA	454679	1949–2007	19	40
	Plummer 3 WSW	ID	107188	1949–2007	31	28
	Pullman 2 NW	WA	456789	1949–2007	18	41
	Sandpoint Exp Stn	ID	108137	1960–2007	19	29
	Spokane Intl AP	WA	457938	1949–2007	0	59
Vancouver	Colton	OR	351735	1949–2007	11	48
	Cougar 4 SW	WA	451759	1949–2007	23	36
	Goble 3 SW	OR	353340	1949–2007	19	40
	Gresham	OR	353521	1949–2007	21	38
	Longview	WA	454769	1955–2007	21	32
	Portland Intl AP	OR	356751	1949–2007	0	59
	Sauvies Island	OR	357572	1949–2007	11	48

precipitation by dividing the precipitation record from each region into two 25-year periods (1956–1980 and 1981–2005). Although we also investigated a finer division of the data into five 10-year periods, the results were statistically inconclusive and so are not reported here.

For each of the two 25-year periods, design storm magnitudes were determined at Seattle–Tacoma (SeaTac), Spokane, and Portland International Airports based on the regional growth curves and the means at those stations. A jackknife method (Efron 1979), whereby one year of record was removed at a time and growth curves refitted, was then used to provide uncertainty bounds about the fitted GEV distributions. Changes in design storm magnitudes were determined by comparing the distributions from each period. Statistical significance for differences in distributions was determined using the Kolmogorov–Smirnov test, for differences in means using the Wilcoxon rank-sum test, and for trends in the entire time series using the Mann–Kendall test, all at a two-sided significance level of 0.05. None of these tests allowed for autocorrelation in the time series, which were all found to be serially independent using a method described in Wallis et al. (2007).

The results indicate an ambiguous collection of changes in extreme precipitation over the last half-century throughout the state. Table 2 presents changes in mean annual maxima between the two time periods, which generally are about the same magnitude of change seen in the 2-year events. Changes at Seattle–Tacoma Airport were consistently positive, with the greatest increases at the 24-h and 2-day durations. Changes at Spokane were mixed, while changes at Vancouver were mostly negative, with the notable exception of the 1- and 24-h durations. None of the changes were found to be statistically significant, however, with the exception of the 2-day and (possibly) 24-h durations at Seattle–Tacoma Airport, and even these significant results most likely would not pass a multiple comparison test.

A breakdown of changes by return period is provided for the 1- and 24-h durations in Table 3, so chosen because of their relevance to urban stormwater infrastructure as indicated in Section 1. Included in the table are estimated return periods of the 1981–2005 events that are equal in magnitude to the 1956–1980 events having the return periods indicated in the first column. Rainfall frequency curves that illustrate the

Table 2 Changes in average annual maxima between 1956–1980 and 1981–2005, as determined by the regional frequency analysis at Seattle–Tacoma, Spokane, and Portland Airports, expressed as a percentage of the 1956–80 mean annual maximum

	SeaTac (%)	Spokane (%)	Portland (%)
1-h	+8.1	−0.3	+4.6
2-h	+10.6	−4.4	−5.1
3-h	+14.8	+1.2	−6.4
6-h	+13.5	+1.5	−7.9
12-h	+19.6	+16.0	−4.8
24-h	+25.6	+7.9	+2.3
2-day	**+23.1**	+3.8	−6.3
5-day	+14.1	−9.5	−4.8
10-day	+7.9	−3.1	−9.4

SeaTac 2-day **+ 23.1%** KS 0.118 **rs 0.019** **MK 0.031**

Changes that are significant for a two-sided α of 0.05 are indicated in bold, with Kolmogorov–Smirnov, Wilcoxon rank-sum, and Mann–Kendall p-values provided at bottom

Table 3 Distribution of changes in fitted 1- and 24-h annual maxima from 1956–1980 to 1981–2005 at Seattle–Tacoma, Spokane, and Portland Airports

Return period (years)	1-h Storm			24-h Storm		
	SeaTac	Spokane	Portland	SeaTac	Spokane	Portland
2	+4.8%	+6.5%	+3.5%	+22.9%	+4.9%	−2.9%
	1.8	*1.7*	*1.8*	*1.3*	*1.7*	*2.2*
5	+4.3%	+1.5%	+3.6%	+29.4%	+6.2%	+4.3%
	4.3	*4.7*	*4.3*	*2.1*	*3.8*	*4.2*
10	+5.8%	−4.1%	+4.2%	+32.1%	+8.2%	+9.8%
	8.0	*11.9*	*8.2*	*3.1*	*6.5*	*6.6*
25	+9.1%	−12.6%	+5.4%	+34.3%	+11.5%	+17.7%
	17.3	*47.9*	*19.0*	*5.7*	*12.8*	*11.5*
50	+12.6%	−19.3%	+6.7%	+35.2%	+14.5%	+24.2%
	30.3	*155.0*	*35.6*	*9.3*	*20.5*	*17.1*
Average	+8.1%	−0.3%	+4.6%	+25.6%	+7.9%	+2.3%
KS	*0.821*	*0.154*	*0.225*	*0.208*	*0.604*	*0.393*
rank-sum	*0.509*	*0.303*	*0.208*	*0.051*	*0.525*	*0.318*
MK	*0.174*	*0.927*	*0.126*	*0.119*	*0.546*	*0.287*

Numbers in italics represent the return periods of the 1981–2005 events that are equal in magnitude to the 1956–1980 events having the return periods indicated in the first column. As an example, for the 1-h storm at SeaTac, the 25-year event from 1956 to 1980 [having a 4% (1/25) chance of occurring in any given year] became a 17.3-year event from 1981 to 2005 [having a 6% (1/17.3) chance of occurring in any given year]. Average changes across all return periods are provided at the bottom, matching those reported in Table 2. None of the changes were found to be significant for a two-sided α of 0.05

changes in 1- and 24-h durations listed in Table 3 are shown in Fig. 2. Shaded regions represent uncertainty bounds as determined by jackknifing the historical data. It is important to note that these uncertainty bounds do not necessarily indicate statistical significance or nonsignificance in changes.

3.2 Precipitation event analysis

In addition to changes in extreme precipitation frequency distributions, it is also useful to estimate trends in total annual precipitation and to determine whether such trends (if significant) are due to changes in storm frequency, storm intensity, or both. An analysis to determine these trends was performed on the NCDC precipitation data by adapting the method of Karl and Knight (1998), which requires a continuous precipitation record with an unchanging level of precision for its application. Thus, we used the single station in each of the urban areas analyzed in the previous section with the most complete record: the airport gauges at Seattle–Tacoma, Spokane, and Portland. Each had a common period of record from January 1, 1949 to December 31, 2007, for a total of 59 years, with a constant precision of 0.254 mm (0.01 in.) throughout.

The central concept in this approach is that once trends in total annual precipitation are determined, the relative influence of changes in event frequency and changes in event intensity can be identified. Trends in event frequency can be determined by defining a precipitation event as any nonzero accumulation over a specified time interval and tallying their number in each period. The remainder of the trends in total annual precipitation can then be attributed to the trends in event

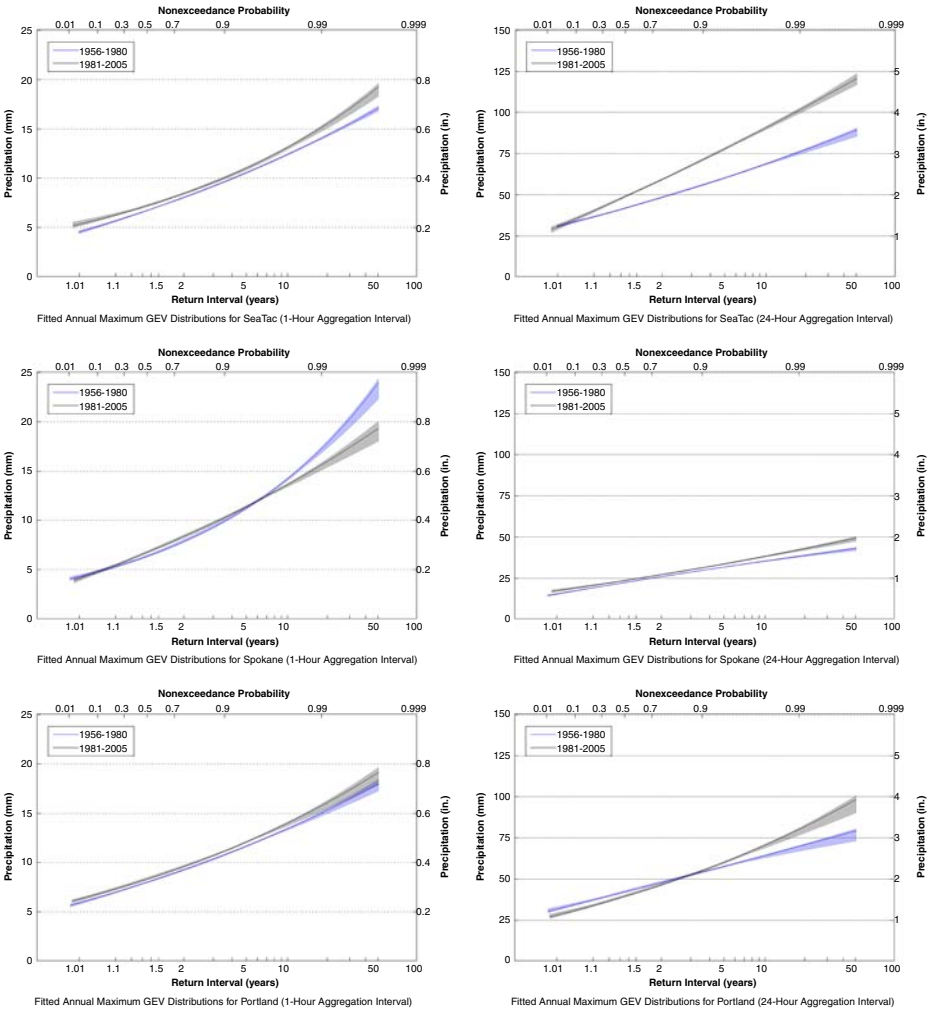

Fig. 2 Changes in fitted 1- and 24-h annual maximum distributions from 1956–1980 to 1981–2005. Uncertainty bounds as determined by the jackknife method are indicated by the *shaded areas*. None of the changes were found to be statistically significant at a two-sided α of 0.05, although the Wilcoxon rank-sum statistic for 24-h distributions at SeaTac was statistically significant at a two-sided α of 0.10. Changes at specific return periods are provided in Table 3

intensity, defined as the amount of precipitation in a given event. The approach provides the additional advantage of determining whether changes were due to trends in light precipitation events, trends in heavy precipitation events, or both. This is a consequence of partitioning each rainfall record into multiple intervals based on event magnitude. We defined an event as any measurable precipitation over a 24-h period (midnight-to-midnight), with the implicit assumption that any day with nonzero precipitation is a single "event".

The analysis was performed by first calculating both the total precipitation and the number of "events" for each year (as defined above), ranking those events from

lowest to highest, and dividing them into 20 class intervals that each contained 1/20 of the total number of events for that year. Thus the first class interval was assigned the 5% of events with the lowest daily totals, the second class interval was assigned the 5% of events with the next lowest daily totals, and so on. For each class, the average long-term precipitation per event (event intensity) was then calculated, and the trend in precipitation due to the trend in event frequency was calculated as:

$$b_e = \overline{P_e}\, b_f$$

where $\overline{P_e}$ is the average long-term event intensity and b_f is the percent change in the frequency of events, as determined by the slope of the linear regression line through a scatter plot of number of events vs. year. The trend in precipitation due to the trend in the annual intensity of events was then calculated as a residual using the expression:

$$b_i = b - b_e$$

where b is the percent change in total precipitation, as determined by the slope of the linear regression line through a scatter plot of total precipitation versus year. Median and highest precipitation events were calculated regardless of class for each year, and trends again were determined by the slopes of their respective regression lines. All trends were divided by average values and multiplied by the 59-year period of analysis.

Results of the analysis are summarized at the annual level for all three stations in Table 4. Trends were tested for significance using the Mann–Kendall test at a two-sided significance level of 0.05. Although none were found to be significant, trends were consistently negative for total precipitation and event frequency, and mostly negative for event intensity. As an example, at Spokane, total annual precipitation has decreased by 13.0% since 1949; 11.9% of this decrease was due to a decrease in event frequency, and the remaining 1.1% of this decrease was due to a decrease in

Table 4 Results of the precipitation event analysis from 1949 to 2007

	SeaTac	Spokane	Portland
Average annual number of events	154.5	110.2	152.1
Average annual precipitation	970 mm (38.2 in.)	419 mm (16.5 in.)	930 mm (36.6 in.)
Trend in annual precipitation	−8.9%	−13.0%	−8.3%
MK	*0.219*	*0.055*	*0.202*
…due to trend in event frequency	−9.3%	−11.9%	−2.6%
MK	*0.056*	*0.052*	*0.843*
…due to trend in event intensity	+0.4%	−1.1%	−5.7%
MK	*0.628*	*0.433*	*0.239*
Trend in annual median event intensity	+4.6%	−1.4%	−2.7%
MK	*0.917*	*0.437*	*0.420*
Trend in annual maximum event intensity	+39.0%	+9.1%	−2.3%
MK	*0.174*	*0.527*	*0.798*

Trends in annual precipitation are provided for the 59-year period as a percentage of the average annual precipitation, as are the portions of these trends due to trends in event frequency and event intensity. Trends in annual median and maximum event intensity are provided as a percentage of their respective long-term averages. Mann–Kendall p-values are provided in italics; none of the trends were found to be significant at a two-sided α of 0.05. An event is defined as any day with measurable (nonzero) precipitation

event intensity. Trends in median event intensity were mixed, however, while trends in maximum event intensity were mostly positive.

Distributions of annual trends by class are shown in Fig. 3, with the class interval containing the smallest 5% of events to the left of each graph and the class interval containing the largest 5% of events (i.e., extreme events) to the right. The sums of the trends in each class equal the cumulative values reported in Table 4. At Seattle–Tacoma Airport, for example, despite mostly negative trends in intensity for the lowest 19 class intervals, a relatively large increasing trend in the intensity of the extreme class interval caused the cumulative trend for intensity to be slightly positive. A closer inspection of the data behind these results at Seattle–Tacoma Airport revealed that 3 of the 4 highest 1-day totals since 1949 have occurred in the last five years.

3.3 Exceedance-over-threshold analysis

In addition to the regional frequency and precipitation event analyses, examining the number of events exceeding given thresholds (e.g., multiples of 2.54 mm [0.1 in.])

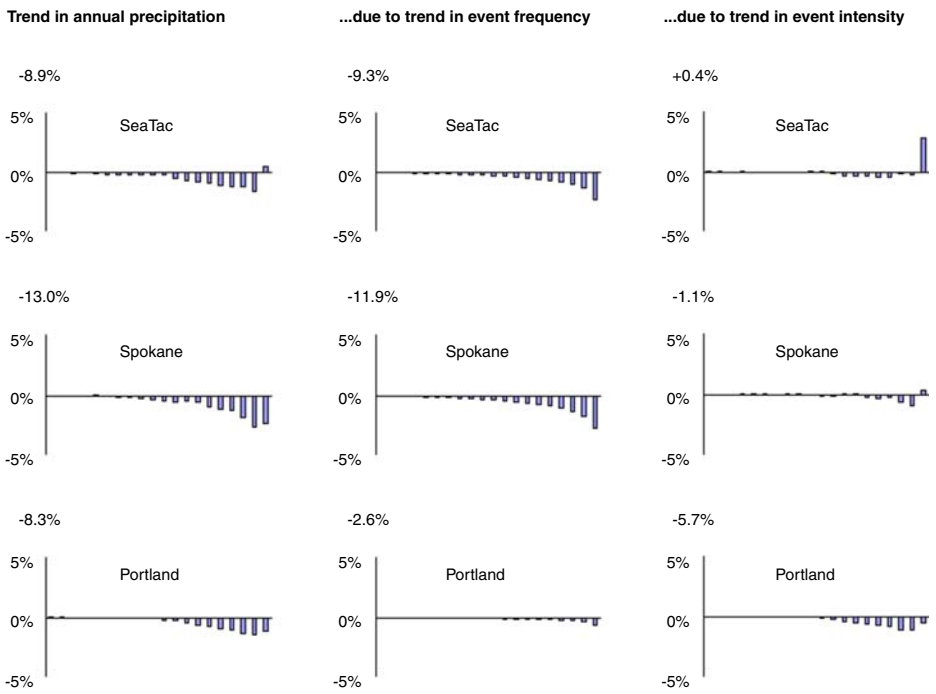

Fig. 3 Distribution of trends reported in Table 4. *At left* are trends in annual precipitation; *at center*, the portion of the trends in annual precipitation due to trends in event frequency; *at right*, the portion of the trends in annual precipitation due to trends in event intensity. An event is defined as any day with measurable (nonzero) precipitation. Trends for individual class intervals are represented by the *bars in each graph*, with the class interval containing the smallest 5% of events *at left* and the class interval containing the largest 5% of events *at right*. *Values above each graph* show cumulative trends across all 20 class intervals

Table 5 Results of the exceedance-over-threshold analysis from 1949 to 2007

	2.54 mm (0.1 in.)	5.08 mm (0.2 in.)	7.62 mm (0.3 in.)	10.16 mm (0.4 in.)	12.70 mm (0.5 in.)
SeaTac	−10.9%	**−15.0%**	**−15.8%**	−13.1%	−12.4%
MK	*0.094*	***0.039***	***0.045***	*0.148*	*0.161*
Max	121	87	61	46	39
Min	68	40	25	12	9
Spokane	**−14.8%**	−15.1%	−21.2%	−23.9%	−17.7%
MK	***0.022***	*0.123*	*0.074*	*0.168*	*0.244*
Max	76	46	27	17	11
Min	38	19	8	2	2
Portland	−4.2%	−8.8%	**−13.3%**	−16.1%	−18.9%
MK	*0.356*	*0.153*	***0.038***	*0.141*	*0.187*
Max	116	92	69	51	41
Min	65	37	22	14	9

Trends in the annual number of events exceeding the specified thresholds are provided for the 59-year period as a percentage of the average annual number of respective exceedances. Mann–Kendall *p*-values are provided in italics; trends that are significant at a two-sided α of 0.05 are indicated in bold. An event is defined as any day with measurable (nonzero) precipitation

throughout a precipitation record provides more detailed information about historical changes in frequency. Such an "exceedance-over-threshold" analysis, distinct from a peak-over-threshold approach which then uses the magnitudes of these events to estimate design storms, was conducted for the three stations examined in Section 3.2. As in the precipitation event analysis, all recorded nonzero daily precipitation totals were treated as single events, which were summed for each year to determine the number of events exceeding each threshold. Trends were then determined by linear regression of these exceedances against time, and expressed as a percentage of the average annual number of exceedances over the 59-year period. The Mann–Kendall test was used to test for statistical significance at a two-sided significance level of 0.05.

As found in the precipitation event analysis, trends in the frequencies of exceedance (Table 5) were negative across all thresholds, suggesting a modest overall decrease in the number of rain events consistent with the decrease in event frequency found in Section 3.2. Statistically significant trends were found for events exceeding several of the thresholds, such as 5.08 mm (0.2 in.) at Seattle–Tacoma Airport (15% decrease over the 59-year period). This analysis does not consider exceedances of thresholds larger than 12.7 mm (0.5 in.) due to the small numbers of these that occur annually, which preclude any meaningful interpretation of trends in more extreme events.

4 Modeled trends in future extreme precipitation

Urban watersheds are small and commonly have rapid surface flow paths for runoff, thereby responding quickly to even short-duration events (Leopold 1968). Their discharge records reflect the influence of individual storm cells and localized bands of high-intensity rainfall, which can sometimes produce runoff responses that vary greatly over just a few kilometers (Gerstel et al. 1997). Thus the raw output from

global climate models (GCMs), on which most assessments of future climate are based, is not directly useable because the model grid resolution (100 s of km) is much too coarse. For this reason, we instead used the two RCM simulations reported by Salathé et al. (2010) that produced downscaled GCM output at hourly aggregations with spatial resolutions of 20 and 36 km (12.4 and 22.3 miles; see Leung et al. 2006; Salathe et al. 2008, 2010 for details). Although these spatial and temporal scales are not ideal for capturing the behavior of urban runoff response, the use of RCM simulations to estimate annual maximum series of precipitation (as opposed to peak-over-threshold extremes only) represents a significant advance in understanding precipitation at the local scales at which watersheds respond to intense rainfall.

The two RCM simulations use different IPCC (2007b) GCM outputs as their boundary conditions. Because the GCMs each predict future climate differently, and also use slightly different global emissions scenarios, it is expected that they will also differ in their projections of future climate. Ideally, a multimodel ensemble at the regional scale, which would parallel that used for regional hydrologic analysis (e.g., Vano et al. 2010a, b), would be available for our analyses. At present, however, this strategy is not computationally feasible (each of the two RCM simulations required several months of computer time). Thus, the results presented here can offer a sense of the likely direction and general magnitude of future changes in precipitation extremes, but reducing their substantial uncertainties must await additional RCM simulations that can be linked to the many other GCMs presently in existence.

4.1 RCM summary

The two GCMs that were used to provide boundary conditions for the RCM simulations were the Community Climate System Model version 3.0 (CCSM3) with the IPCC A2 emissions scenario, and the Max Planck Institute's ECHAM5 with the IPCC A1B emissions scenario (Table 6). During the first half of the 21st century, atmospheric CO_2 concentrations are similar in both the A2 and the A1B emissions scenarios, and so differences in the RCM simulation results are mostly due to differences in the GCMs. Differences in spatial resolution may also influence the results in ways that remain to be systematically explored. Both CCSM3 and ECHAM5 are considered to be in the middle of the range of existing GCMs in their projections of precipitation for the Pacific Northwest (Mote et al. 2005).

The RCM used to downscale both GCMs was the Weather Research and Forecasting (WRF) mesoscale climate model (http://www.wrf-model.org) developed at the National Center for Atmospheric Research (NCAR). The CCSM3/A2 WRF simulation was performed on a grid spacing of 20 km (12.4 miles), while the

Table 6 Summary of emission scenarios, GCMs, and geographic coordinates of the downscaled precipitation records used for this study

IPCC Emissions Scenario	Global Circulation Model (GCM)	Regional Climate Model (RCM)	RCM grid spacing for Washington State simulation	Lat-Long Coordinates of RCM output used for hydrologic modeling (see Fig. 4)	
A2[a]	CCSM3	WRF	20 km (12.4 miles)	47.525 °N	122.287 °W
A1B[b]	ECHAM5	WRF	36 km (22.3 miles)	47.500 °N	122.345 °W

[a] A2 simulations performed by Pacific Northwest National Laboratories

[b] A1B simulations performed by UW-CIG

ECHAM5/A1B WRF simulation had a grid spacing of 36 km (22.3 miles). Both model simulations covered the time periods 1970–2000 (the "historical" period) and 2020–2050 (the "future" period), from which hourly precipitation data were extracted. Annual maxima were derived from these "raw" data at grid points near each of the three airports in the three urban regions (Puget Sound, Spokane, and Vancouver–Portland). Statistical significance for differences in distributions was determined using the Kolmogorov–Smirnov test, for differences in means using the Wilcoxon rank-sum test, and for trends in the entire time series using the Mann–Kendall test, all at a two-sided significance level of 0.05.

Changes in average annual maxima between the two time periods are reported in Table 7. While there was a greater number of increases than decreases, the magnitudes of the changes vary considerably across locations and simulations. Statistically significant changes were found for the Puget Sound region for both simulations, for Spokane for the CCSM3/A2 simulation for 3-h storms and for the ECHAM5/A1B simulation for 24-h storms, and for Vancouver–Portland for the CCSM3/A2 simulation for 1-, 2-, and 3-h storms. Curiously, the intensities of shorter duration storms for Puget Sound and Spokane are projected to increase under the CCSM3/A2 simulations but decrease for the ECHAM5/A1B simulations.

A closer inspection of results for the CCSM3/A2 simulations revealed that, particularly for the Puget Sound region, the vast majority of modeled future annual maxima are projected to occur in the month of November, a finding that was not replicated in the ECHAM5/A1B simulations. Quality control checks demonstrated that these elevated November projections were indeed present in the underlying

Table 7 Changes in the average modeled empirical annual maxima from 2020 to 2050 relative to the average modeled empirical annual maxima from 1970 to 2000, using raw RCM data

	CCSM3/A2			ECHAM5/A1B		
	SeaTac	Spokane	Portland	SeaTac	Spokane	Portland
1-h	**+16.2%**	+10.3%	**+10.5%**	−4.6%	−6.6%	+2.1%
2-h	**+16.9%**	+5.9%	**+7.0%**	−4.3%	−6.4%	+3.9%
3-h	**+17.5%**	**+6.3%**	**+6.5%**	−4.0%	−5.8%	+2.9%
6-h	**+18.3%**	+5.4%	+3.6%	+3.6%	−1.7%	+1.2%
12-h	+15.9%	+5.5%	−0.5%	+9.1%	+12.1%	+2.1%
24-h	+18.7%	+3.9%	+4.8%	**+14.9%**	**+22.2%**	+2.0%
2-day	+11.2%	+4.2%	+2.0%	**+13.8%**	+16.0%	+3.1%
5-day	+6.3%	+3.2%	+9.0%	+12.2%	+8.8%	+4.6%
10-day	+9.0%	+2.3%	+7.5%	+7.2%	+8.9%	+11.5%

CCSM3/A2	SeaTac	1-h	**+16.2%**	**KS 0.014**	**rs 0.011**	**MK 0.015**
CCSM3/A2	SeaTac	2-h	**+16.9%**	KS 0.062	**rs 0.013**	**MK 0.027**
CCSM3/A2	SeaTac	3-h	**+17.5%**	**KS 0.030**	**rs 0.007**	**MK 0.020**
CCSM3/A2	SeaTac	6-h	**+18.3%**	KS 0.120	**rs 0.019**	MK 0.116
CCSM3/A2	Spokane	3-h	**+6.3%**	KS 0.120	rs 0.128	**MK 0.044**
CCSM3/A2	Portland	1-h	**+10.5%**	KS 0.120	**rs 0.044**	**MK 0.004**
CCSM3/A2	Portland	2-h	**+7.0%**	KS 0.062	rs 0.076	**MK 0.007**
CCSM3/A2	Portland	3-h	**+6.5%**	KS 0.062	rs 0.078	**MK 0.009**
ECHAM5/A1B	SeaTac	24-h	**+14.9%**	**KS 0.006**	**rs 0.022**	**MK 0.045**
ECHAM5/A1B	SeaTac	2-day	**+13.8%**	**KS 0.030**	**rs 0.034**	MK 0.072
ECHAM5/A1B	Spokane	24-h	**+22.2%**	**KS 0.013**	**rs 0.023**	**MK 0.049**

Statistically significant changes are indicated in bold and provided at bottom, as in Table 2

GCM, but that they originated from the one ensemble member with the greatest divergence from the ensemble mean, which indicates more modest changes in autumn precipitation. Thus, these particular results must be interpreted as the combined influence of systematic climate change and internal climate variability. This result emphasizes the need to utilize a broader cross-section of GCMs and ensemble members in a more comprehensive analysis, notwithstanding the considerable computational expense that this implies. For a more complete discussion, see Salathé et al. (2010).

As a means of further interpreting the calculated changes, we performed a minimum detectable difference (MDD) analysis for each model run/duration combination. The MDD is the smallest statistically significant change that can be detected by a test of a specified power, given the sample size and underlying distribution of the observations (characterized in our case by the mean and variance). For this analysis, we assumed that the population was normally distributed, with changes estimated using the Student's *t*-statistic to approximate the MDD (see, e.g., Lettenmaier 1976, who also shows that results of the Mann–Kendall test are similar to those of the *t*-test when the underlying distribution is normal). We first determined the post-hoc power of the *t*-test assuming a two-sided α of 0.05 and the actual sample's combined size, variance, and detected change in average annual maxima (as reported in Table 7). Next, we calculated the MDD of the *t*-test, again assuming a two-sided α of 0.05 and the actual sample's combined size and variance, but this time with the power taken to be 0.5. Finally, we estimated the combined sample size that would be required to demonstrate statistical significance for the detected change in average annual maxima, given the sample's variance, and assuming a two-sided α of 0.05 and power of 0.5.

The results of the MDD analysis (Table 8) offer further explanation for the patterns presented in Table 7. With the exception of the CCSM3/A2 simulation at Seattle–Tacoma Airport, which resulted in a greater number of statistically significant results for the reasons discussed above, the majority of post-hoc powers were determined to be largely deficient. In most cases, MDDs were likewise determined to be greater than the detected changes in average annual maxima provided in Table 7. The underlying reason is that the sample variances were too large for the sample sizes available. Stated otherwise, most of the required sample sizes were considerably larger than the 62 years of simulations available for our analyses.

4.2 Bias correction and statistical downscaling (BCSD)

Although the raw output from the RCM provides a broadly recognizable pattern of rainfall, even a cursory comparison of simulated and gauged records shows obvious disparities in both the frequency of rainfall events and the total amount of recorded precipitation. For example, from 1970 to 2000, the CCSM3/A2 simulation at the grid center closest to Seattle–Tacoma Airport resulted in 11,734 h of nonzero precipitation for a total of 5,720 mm (225 in.) during the month of January (average of 379 h and 185 mm [7.3 in.]), while the Seattle–Tacoma Airport gauge recorded only 4,144 h of nonzero precipitation for a total of 4,110 mm (162 in.; average of 134 h and 133 mm [5.2 in.]). Thus, if the RCM data are to be used as forcings for a hydrologic model, they must first be bias-corrected. We describe a procedure for doing so in the remainder of this section, which focuses on the central Puget Sound region.

Table 8 Results of the MDD analysis

		CCSM3/A2			ECHAM5/A1B		
		SeaTac	Spokane	Portland	SeaTac	Spokane	Portland
1-h	power	**0.63**	0.14	**0.30**	0.07	0.11	0.05
	MDD	**13.9%**	22.9%	**14.2%**	17.1%	17.6%	13.2%
	n_{min}	**56**	138	**84**	228	160	386
2-h	power	**0.64**	0.08	**0.17**	0.07	0.11	0.09
	MDD	**14.4%**	20.2%	**13.8%**	17.0%	16.6%	12.8%
	n_{min}	**54**	208	**122**	236	158	198
3-h	power	**0.65**	**0.09**	**0.15**	0.07	0.11	0.07
	MDD	**14.6%**	**19.2%**	**13.7%**	16.5%	14.9%	12.4%
	n_{min}	**52**	**186**	**128**	250	158	260
6-h	power	**0.61**	0.08	0.07	0.07	0.04	0.04
	MDD	**16.1%**	19.5%	14.2%	14.6%	14.1%	11.7%
	n_{min}	**56**	218	236	244	486	590
12-h	power	0.44	0.08	0.03	0.25	0.33	0.05
	MDD	17.2%	19.7%	15.9%	13.7%	15.6%	12.6%
	n_{min}	68	220	1826	92	80	360
24-h	power	0.52	0.06	0.09	**0.48**	**0.61**	0.05
	MDD	18.3%	20.3%	15.1%	**15.2%**	**19.4%**	13.7%
	n_{min}	62	316	192	**64**	**54**	408
2-day	power	0.28	0.06	0.05	**0.34**	0.40	0.06
	MDD	15.9%	19.4%	13.6%	**17.5%**	18.5%	15.4%
	n_{min}	88	276	402	**78**	72	302
5-day	power	0.12	0.05	0.27	0.30	0.21	0.08
	MDD	15.6%	17.8%	13.0%	16.7%	14.7%	16.5%
	n_{min}	150	330	90	84	104	220
10-day	power	0.24	0.05	0.22	0.15	0.28	0.25
	MDD	13.9%	16.3%	12.2%	15.4%	12.7%	17.4%
	n_{min}	94	434	100	130	90	94

The top row of each cell is the post-hoc power of a *t*-test assuming a two-sided α of 0.05 and the actual sample's combined size, sample variance, and detected change in average annual maxima, as reported in Table 7. The middle row is the MDD of a *t*-test, again assuming a two-sided α of 0.05 and the actual sample's combined size and variance, with power of 0.5. The bottom row is the combined sample size that would be required for the detected change in average annual maxima to be statistically significant, given the sample's variance, and assuming a two-sided α of 0.05 and power of 0.5. Results corresponding to detected changes that were statistically significant are indicated in bold

Methods of removing systematic bias in RCM output are described by Wood et al. (2002) and Payne et al. (2004). We generalized their procedure, which is based on probability mapping as described by Wilks (2006), to apply to precipitation extremes. The objective of the procedure is to transform the modeled data so that they have the same probability distributions as their observed counterpart.

Bias correction was applied to the simulation record for the grid point from each of the two downscaled hourly WRF time series (1970–2000 and 2020–2050) that was closest to Seattle–Tacoma Airport (Fig. 4). For the RCM run forced by the CCSM3/A2 simulation (hereafter referred to as the "CCSM3" run), the grid

Fig. 4 Locations of the two grid points used for BCSD, shown in relation to SeaTac Airport and the Thornton Creek and Juanita Creek watersheds (see Section 5). Figure: Robert Norheim

point employed was 47.525° N, 122.287° W, corresponding to a location about 9 km (5.6 miles) NNE of Seattle–Tacoma Airport. For the RCM run forced by the ECHAM5/A1B simulation (hereafter referred to as the "ECHAM5" run), the grid point employed was 47.500° N, 122.345° W, corresponding to a location about 7 km (4.3 miles) NNW of Seattle–Tacoma Airport. For purposes of comparison, a separate bias correction was performed for each run at their next grid point to the south; results were very similar and are not reported here.

The first step in the procedure was to truncate simulated data for the 1970–2000 period so that each month had the same number of nonzero hourly values as the observed data from the Seattle–Tacoma Airport gauge, which were the same data used in the historical analyses described in Section 3. This was done to correct for oversimulation by the RCM of small amounts (sometimes termed the "climate model drizzle problem"). Simulated data for the future period (2020–2050) were similarly truncated, using the same threshold hourly values resulting from matching the number of nonzero past values to that which was observed. Thus, using the example provided above, the 7,590 h (i.e., 11,734–4,144 h) containing the smallest amounts of nonzero precipitation were eliminated from the 1970–2000 simulated record for the month of January, coinciding with a truncation threshold of 0.3 mm (0.012 in.). Any hour during the month of January during the 2020–2050 simulated

record with a nonzero precipitation of less than 0.3 mm (0.012 in.) was also eliminated (6,824 out of 10,322 h).

Bias correction was then achieved by replacing RCM values with values having the same nonexceedence probabilities, with respect to the observed climatology, that the original RCM values had with respect to the RCM climatology. The procedure was first performed at a monthly time interval to ensure that the dramatic seasonal differences that characterize rainfall in western Washington were preserved and represented accurately. Monthly totals were calculated (by year), and the Weibull plotting position was employed to map those totals from the simulated empirical cumulative distribution function (eCDF) to monthly totals from the observed eCDF. Next, simulated hourly values were rescaled to add up to the new monthly totals. The procedure was then repeated; the new hourly values were mapped from their eCDF to the hourly values from the observed eCDF and once again rescaled to match the monthly totals derived in the first mapping step. Values that fell outside the range of the simulated climatology, but within 3.5 standard deviations of the climatological mean, were corrected by assuming a lognormal distribution. Those that fell outside of 3.5 standard deviations of the climatological mean were corrected by scaling the mean of the observed climatology by its ratio with the mean of the simulated climatology.

The resulting eCDFs for historical and future climate were tested for significance of differences using the Kolmogorov–Smirnov, Wilcoxon rank-sum, and Mann–Kendall tests at a two-sided α of 0.05. Overall, average biases in empirical annual maxima were reduced from −22.2% to +3.1% for the ECHAM5 run, and from +9.6% to +2.5% for the CCSM3 run (Table 9). Changes in the raw annual maxima between the 1970–2000 and 2020–2050 periods were largely preserved, although the procedure did have the effect of making some of the changes under the CCSM3 simulation more statistically significant. Under the ECHAM5 run, the corrected empirical annual maxima display a decrease between the two 30-year periods by an average of 5.8 to 6.3% for 1-, 2-, and 3-h durations, and an increase of 2.3 to 14.1% for the remaining durations. For the CCSM3 run, the corrected empirical annual maxima show an increase of 13.7 to 28.7% across all durations.

It is generally recognized that the downscaling problem is more complicated for precipitation extremes than precipitation means, for the intuitive reason that most extreme events tend to be concentrated on very small spatial scales, which are not well represented in climate models. Because the magnitudes of our bias corrections of simulated data is necessarily greater in the tails of the distributions than in the middle, our analysis effectively accounts for this problem. That said, the procedure is not exact, and there are no doubt refinements that can still be made. However, the ranges and medians of the modeled, bias-corrected maxima generally match those of the observed maxima for the historical period (1970–2000), as shown for the 24-h duration in Fig. 5.

5 Prediction of future changes in urban flood extremes

Although our analysis thus far has focused on changes in precipitation across the major urban areas of Washington State, the direct relevance of these changes to stormwater infrastructure is best displayed through predictions of future

Table 9 Results of the bias-correction procedure for both RCM runs at Seattle–Tacoma Airport

	CCSM3/A2				ECHAM5/A1B			
	Bias		Change		Bias		Change	
	Raw	Cor	Raw	Cor	Raw	Cor	Raw	Cor
1-h	−19.2%	−7.3%	**+16.2%**	**+14.3%**	−33.2%	−13.4%	−4.6%	−6.3%
2-h	−2.6%	+4.1%	**+16.9%**	**+22.8%**	−21.2%	+3.9%	−4.3%	−5.8%
3-h	+2.4%	+6.2%	**+17.5%**	**+23.7%**	−17.3%	+11.8%	−4.0%	−6.3%
6-h	+8.8%	+6.6%	**+18.3%**	**+24.3%**	−17.3%	+12.8%	+3.6%	+2.3%
12-h	+12.7%	+4.4%	+15.9%	**+24.2%**	−20.6%	+6.8%	+9.1%	+8.3%
24-h	+11.0%	−1.9%	+18.7%	**+28.7%**	−22.7%	+3.4%	**+14.9%**	**+14.1%**
2-day	+19.4%	−1.1%	+11.2%	**+24.0%**	−22.7%	+1.2%	**+13.8%**	**+14.1%**
5-day	+29.0%	+7.1%	+6.3%	+13.7%	−22.4%	+1.1%	+12.2%	+11.5%
10-day	+25.1%	+4.6%	+9.0%	**+18.0%**	−22.4%	+0.3%	+7.2%	+7.8%
Average	+9.6%	+2.5%	–	–	−22.2%	+3.1%	–	–

CCSM3/A2	1-h (raw)	**+16.2%**	**KS 0.014**	**rs 0.011**	**MK 0.015**	1-h (cor)	**+14.3%**	**KS 0.002**	**rs 0.013**	**MK 0.003**
CCSM3/A2	2-h (raw)	**+16.9%**	KS 0.062	**rs 0.013**	**MK 0.027**	2-h (cor)	**+22.8%**	**KS 0.001**	**rs 0.001**	**MK 0.001**
CCSM3/A2	3-h (raw)	**+17.5%**	**KS 0.030**	**rs 0.007**	**MK 0.020**	3-h (cor)	**+23.7%**	**KS 0.002**	**rs 0.000**	**MK 0.001**
CCSM3/A2	6-h (raw)	**+18.3%**	KS 0.120	**rs 0.019**	MK 0.116	6-h (cor)	**+24.3%**	**KS 0.030**	**rs 0.005**	**MK 0.044**
CCSM3/A2	12-h (raw)	+15.9%	KS 0.216	rs 0.076	MK 0.331	12-h (cor)	**+24.2%**	**KS 0.030**	**rs 0.009**	MK 0.155
CCSM3/A2	24-h (raw)	+18.7%	KS 0.216	rs 0.052	MK 0.291	24-h (cor)	**+28.7%**	**KS 0.013**	**rs 0.003**	MK 0.085
CCSM3/A2	2-day (raw)	+11.2%	KS 0.120	rs 0.143	MK 0.331	2-day (cor)	**+24.0%**	**KS 0.013**	**rs 0.004**	MK 0.099
CCSM3/A2	10-day (raw)	+9.0%	KS 0.216	rs 0.177	MK 0.572	10-day (cor)	**+18.0%**	**KS 0.002**	**rs 0.010**	MK 0.078
ECHAM5/A1B	24-h (raw)	**+14.9%**	**KS 0.006**	**rs 0.022**	**MK 0.045**	24-h (cor)	**+14.1%**	KS 0.062	**rs 0.040**	**MK 0.034**
ECHAM5/A1B	10-day (raw)	**+13.8%**	**KS 0.030**	**rs 0.034**	MK 0.072	10-day (cor)	**+14.1%**	**KS 0.006**	**rs 0.023**	**MK 0.033**

The reported biases are those of the average modeled empirical annual maxima (both raw and corrected) relative to the average observed empirical annual maxima from 1970 to 2000. The reported changes are those of the average modeled empirical annual maxima from 2020 to 2050 relative to the average modeled empirical annual maxima from 1970 to 2000, using both raw and corrected data. Statistically significant changes are indicated in bold with test statistics provided at bottom, as in Table 2

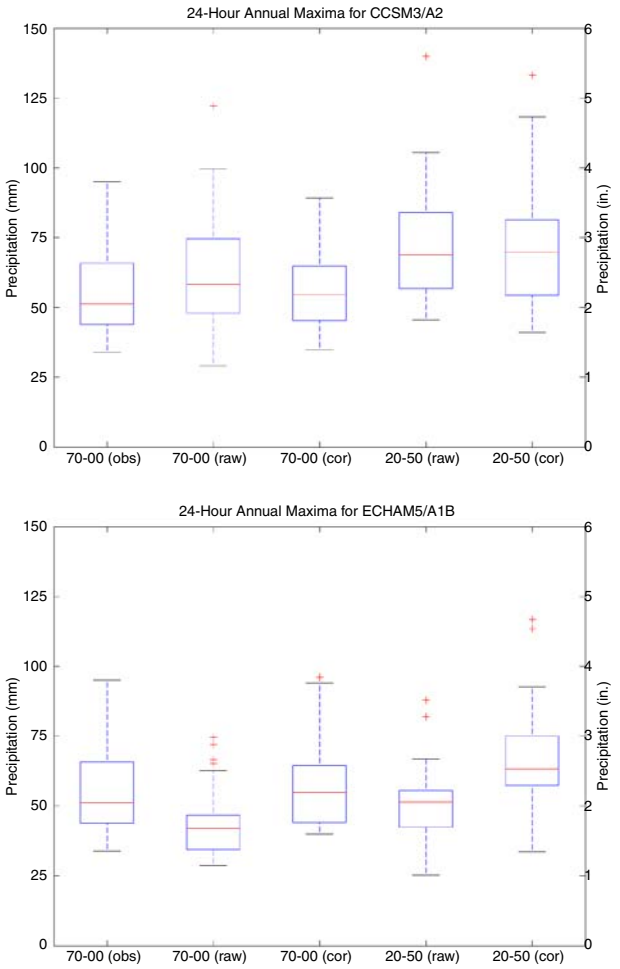

Fig. 5 Box-whisker plots of observed and modeled (raw and bias-corrected) 24-h annual maxima at Seattle–Tacoma Airport for the CCSM3/A1 scenario (*upper*) and the ECHAM5/A1B scenario (*lower*). *Red line* denotes the median, *solid box* denotes the range from 25th to 75th percentiles, and *whiskers* denote the range of the rest of the data. *Plus signs* denote outliers more than 1.5 times the interquartile range from the *top or bottom of the box*

streamflows. As case studies, we selected two Seattle-area watersheds (Fig. 4), Thornton Creek in the City of Seattle and Juanita Creek in the City of Kirkland and adjacent unincorporated King County, because they encompass physical and land-use characteristics typical of the central Puget Lowland. The Thornton Creek watershed is Seattle's largest, with approximately 2870 ha (7090 ac) of mixed commercial and residential land use. Juanita Creek is a mixed-land-use 1760-ha (4350-ac) watershed that drains to the eastern shore of Lake Washington; its land cover is 34% effective impervious with 30% forest cover.

Hydrologic simulations of streamflows in these two watersheds were generated by the Hydrologic Simulation Program-Fortran (HSPF; Bicknell et al. 1996). HSPF, which was developed under contract to and is maintained by the U.S. Environmental Protection Agency, is a lumped-parameter model that simulates discharge at user-selected points along a channel network from a time series of meteorological variables (notably, rainfall, temperature, and solar radiation) and a characterization of hydrologic variables (such as infiltration capacity and soil water-holding capacity)

that are typically averaged over many hectares or square kilometers. HSPF has been widely applied across western Washington since its first regional application in the mid-1980s (King County 1985), and the procedures for model set-up, initial parameter selection, and calibration are well established for the region (Dinicola et al. 1990, 2001).

The BCSD precipitation data for the periods 1970–2000 and 2020–2050 were input to HSPF to reconstitute historical streamflows and predict future streamflows in the Thornton Creek and Juanita Creek watersheds using the RCM grid points previously discussed (see Section 4.2; Table 6 and Fig. 4). Because the inputs to the hydrologic model for the two periods differed only in precipitation, any attribute of an altered hydrologic response that is not driven predominantly by rainfall (e.g., the dependence of low-flow extremes on evapotranspiration rates) would not be plausibly represented and has not been explored here. These two case studies, however, offer some guidance as to whether predicted runoff changes in urban and suburban areas present any critical areas of concern for stormwater managers.

5.1 Results

To parallel the approach of the BCSD analysis, HSPF was first used to evaluate differences between 1970–2000 simulated flows resulting from forcing HSPF with the historical rainfall record and the BCSD rainfall. Results from both the Thornton Creek and Juanita Creek modeling runs suggest streamflow biases of the same magnitude or less than those from the direct comparison of observed and simulated rainfall records (see Tables 10, 11, 12 and Fig. 6). For the exploratory purposes that motivated the modeling, these differences were judged acceptable.

Streamflows were then simulated for both watersheds and each of the two RCM runs using the BCSD rainfall for the periods 1970–2000 and 2020–2050. Log-Pearson type 3 distributions were fitted to the resulting annual maxima, as recommended by US federal agencies for flood frequency analyses (IACWD 1982), and changes were tested for statistical significance using the Kolmogorov–Smirnov, Wilcoxon rank-sum, and Mann–Kendall tests at a two-sided α of 0.05. Results at the mouths of both watersheds (Tables 10 and 11) indicate increases in streamflows for both RCM runs at all recurrence intervals. While these increases are smaller at the mouth of Juanita Creek, this is most likely the consequence of an extensive wetlands complex that attenuates peak flows in that watershed.

Despite this relative uniformity, however, not every scenario is equally consistent. Statistically significant results using CCSM3-generated precipitation are systematically greater than those using ECHAM5, which are not statistically significant. Even the relatively large increases at Thornton Creek under ECHAM5 are insignificant, due to the large variance present in those particular data. In addition, in the HSPF results for Kramer Creek, a 45-ha (110-ac) mixed commercial and residential subwatershed that constitutes less than 2% of the Thornton Creek watershed area, simulated changes in peak flow differ in sign between the two scenarios. For the CCSM3-driven simulations, 2-year through 50-year peak flows are projected to rise by as much as 25% while the ECHAM5-driven simulations mostly indicate small declines (Table 12). Although they constitute only a single example, these substantially different results suggest that the present state of understanding in the

Table 10 Comparisons of HSPF-simulated annual maximum streamflows at the mouth of Juanita Creek, as forced by bias-corrected data for 1970–2000 and 2020–2050 from each of the two RCM runs

Return interval (years)	CCSM3-WRF				ECHAM5-WRF			
	Peak flow quantiles 1970–2000	% Diff from Obs	Peak flow quantiles 2020–2050	Change from 1970–2000	Peak flow quantiles 1970–2000	% Diff from Obs	Peak flow quantiles 2020–2050	Change From 1970–2000
2	6.51 (230)	+6%	8.18 (289)	+**26**%	6.34 (224)	+3%	7.14 (252)	+13%
5	8.07 (285)	+3%	10.14 (358)	+**26**%	8.13 (287)	+4%	9.00 (318)	+11%
10	9.00 (318)	+1%	11.33 (400)	+**26**%	9.34 (330)	+4%	10.14 (358)	+9%
25	10.14 (358)	−3%	12.77 (451)	+**26**%	10.85 (383)	+4%	11.47 (405)	+6%
50	10.93 (386)	−5%	13.82 (488)	+**26**%	12.01 (424)	+4%	12.40 (438)	+3%
KS				***0.030***				*0.216*
rank-sum				***0.002***				*0.147*
MK				***0.040***				*0.056*

Streamflows are given in cubic meters per second (cubic feet per second in parentheses). Percent differences indicated are with respect to HSPF-simulated annual maximum streamflows as forced by observed data for 1970–2000. Statistically significant changes are indicated in bold

Table 11 Comparisons of HSPF-simulated annual maximum streamflows at the mouth of Thornton Creek, as forced by bias-corrected hourly precipitation data for 1970–2000 and 2020–2050 from each of the two RCM runs

Return interval (years)	CCSM3-WRF				ECHAM5-WRF			
	Peak flow quantiles 1970–2000	% Diff from Obs	Peak flow quantiles 2020–2050	Change from 1970–2000	Peak flow quantiles 1970–2000	% Diff from Obs	Peak flow quantiles 2020–2050	Change from 1970–2000
2	3.34 (118)	+17%	5.30 (187)	+**59**%	3.03 (107)	+6%	3.79 (134)	+25%
5	5.27 (186)	+14%	8.27 (292)	+**57%**	4.90 (173)	+6%	6.37 (225)	+30%
10	6.74 (238)	+10%	10.31 (364)	+**53**%	6.43 (227)	+5%	8.38 (296)	+30%
25	8.83 (312)	+6%	12.97 (458)	+**47**%	8.75 (309)	+5%	11.30 (399)	+29%
50	10.56 (373)	+2%	14.98 (529)	+**42**%	10.79 (381)	+5%	13.73 (485)	+27%
KS				***0.003***				*0.951*
rank-sum				***0.001***				*0.624*
MK				***0.005***				*0.399*

Statistically significant changes are indicated in bold

Table 12 Comparisons of HSPF-simulated annual maximum streamflows at the mouth of Kramer Creek, as forced by bias-corrected hourly precipitation data for 1970–2000 and 2020–2050 from each of the two RCM runs

Return interval (years)	CCSM3-WRF				ECHAM5-WRF			
	Peak flow quantiles 1970–2000	% Diff from Obs	Peak flow quantiles 2020–2050	Change from 1970–2000	Peak flow quantiles 1970–2000	% Diff from Obs	Peak flow quantiles 2020–2050	Change from 1970–2000
2	0.20 (7.0)	+4%	0.25 (8.8)	+**25**%	0.19 (6.6)	−1%	0.19 (6.7)	0%
5	0.24 (8.6)	+4%	0.30 (10.6)	+**25**%	0.24 (8.3)	0%	0.24 (8.3)	0%
10	0.27 (9.5)	+1%	0.33 (11.7)	+**22**%	0.27 (9.4)	0%	0.26 (9.3)	−4%
25	0.30 (10.6)	0%	0.36 (12.8)	+**20**%	0.31 (10.9)	+3%	0.29 (10.4)	−6%
50	0.32 (11.4)	−1%	0.38 (13.5)	+**19**%	0.34 (12.0)	+4%	0.32 (11.2)	−8%
KS				***0.001***				*0.951*
rank-sum				***0.001***				*0.898*
MK				***0.001***				*0.455*

Statistically significant changes are indicated in bold

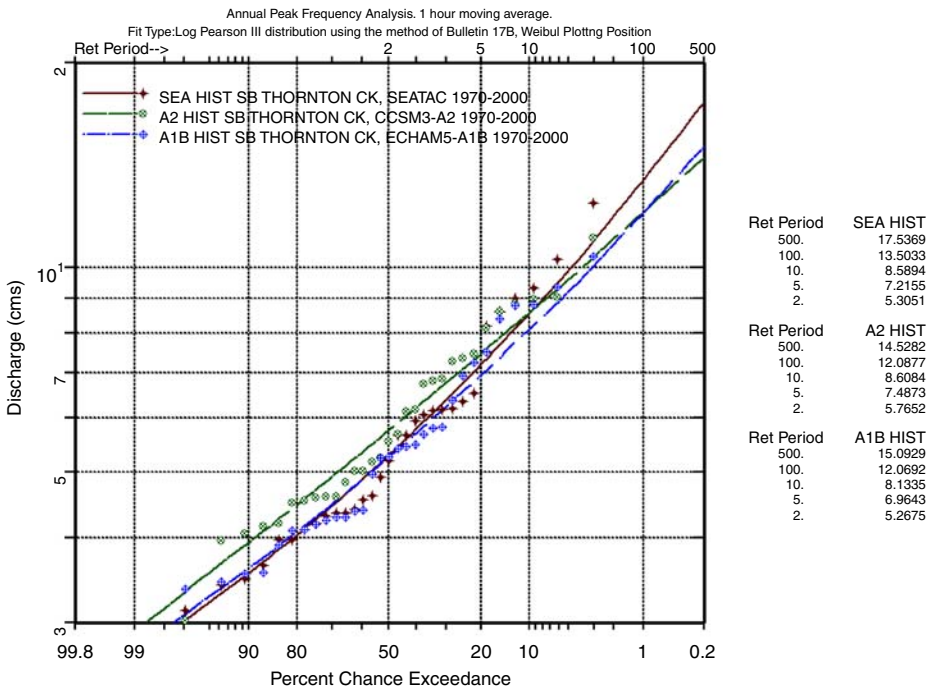

Fig. 6 Example Flood Frequency Curves for the South Branch of Thornton Creek (930-ha [2300-ac] drainage area), comparing HSPF-simulated results for the period 1970–2000 driven by the Seattle–Tacoma Airport rainfall record (*red line and symbols*) with the results driven by the BCSD rainfall from the two alternative climate scenarios (*green and blue*)

implications of projected changes in precipitation extremes is still highly uncertain, at least for small urban drainage basins of this scale.

We explored predicted changes in runoff characteristics for both RCM runs for flow metrics other than peak annual discharge, using selected indices of hydrologic alteration (IHA) that have likely ecological influence (Konrad and Booth 2002; Richter et al. 1996). These include indices that assess the time of year for average or extreme flow events, the frequency and duration of flow pulses, and the rate and frequency of change in flow conditions. In general, these metrics did not change nearly as much as did the peak annual discharge (e.g., Table 10). As an example, the results for high pulse start date at Juanita Creek (Fig. 7) are relatively consistent: only modest differences are apparent between the two scenarios, and very limited differences between the two simulation periods.

In contrast, analysis of a common measure of stream-channel erosivity (aggregate duration of flow above a threshold discharge) indicates systematic changes between the present and future periods. The threshold discharge assumed in this study is 50% of the peak 2-year flow for the period 1970–2000, which has been found to be a regionally credible index value for initiation of sediment transport in an alluvial gravel-bed channel (Booth and Jackson 1997). A single value, derived from the average of the three 1970–2000 simulations, was used as this "threshold discharge" for all duration analyses at a given stream location. Both RCM-driven

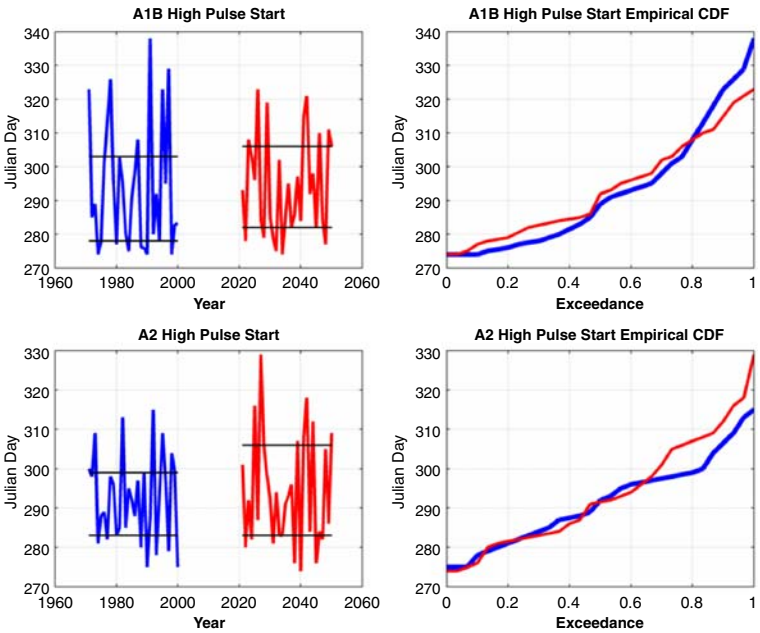

Fig. 7 Example of an IHA metric (high pulse start date) as simulated by the two RCM-based HSPF simulations for the periods 1970–2000 and 2020–2050 at the mouth of Juanita Creek. Differences between models, or between periods, are neither systematic nor particularly large

simulations show consistent increases, with the largest change associated with the smallest watershed area (Table 13). Similar to other results that compare simulated 2020–2050 flows to those for 1970–2000, increases in erosivity predicted using the CCSM3 precipitation dataset are consistently more dramatic than those predicted using the ECHAM5 dataset. In comparison to streamflow simulations driven by the

Table 13 Flow durations for Q > 50% of the 2-year discharge (percent of time exceedance), as predicted by HSPF at four locations along the channel network of Thornton Creek

SeaTac historical	CCSM3-WRF			ECHAM5-WRF		
1970–2000 (%)	1970–2000 (%)	2020–2050 (%)	Change (%)	1970–2000 (%)	2020–2050 (%)	Change (%)
Kramer Creek (45 ha [110 ac])						
0.23	0.28	0.58	+107	0.29	0.51	+76
South Branch Thornton Creek						
0.23	0.28	0.42	+50	0.29	0.34	+17
North Branch Thornton Creek						
0.36	0.45	0.66	+47	0.46	0.56	+22
Thornton Creek nr Mouth (2870 ha [7090 ac])						
0.19	0.24	0.38	+58	0.24	0.30	+25

The first column gives the time of exceedance using the historical record; the 1970–2000 column for each GCM shows the same metric using the BCSD simulated record (with simulation results about 1/3 higher, on average). The column labeled Change is the 2020–2050 value for this metric relative to the 1970–2000 durations using the BCSD rainfall record

historical 1970–2000 rainfall record, however, both RCM-driven simulations consistently overestimate high-flow durations by approximately one-third. Interestingly, the two different RCM-based simulations produce very consistent errors; apparently the bias-correction procedures do not adequately adjust the moderate levels of precipitation intensity that affect this flow statistic.

6 Discussion

Our analyses of historical precipitation yielded largely (statistically) inconclusive trends in extreme precipitation over a range of durations during the past half-century, with substantial differences among the three major metropolitan areas. In the Puget Sound region, statistically significant increases in annual maxima were observed at the 24-h duration, which is the interval most frequently used for the design of stormwater infrastructure. Annual maxima in the other two regions, however, displayed markedly different changes over the last 50 years, with mixed results in the Spokane region and consistently negative changes in the Portland–Vancouver region, none of which were statistically significant. Although prior studies have mostly focused on trends in the frequency of extreme events, and not in intensity as we have done here, these results are consistent with those of Kunkel et al. (1999) and Pryor et al. (2009), both of which found ambiguous trends in the Pacific Northwest, as well as Madsen and Figdor (2007), who found statistically significant upward trends in both Washington and Seattle but mixed trends in Oregon and Idaho.

Modeled trends in future precipitation extremes were generally more consistent than in the historical analyses. Two different GCMs provided the coarse-scale boundary conditions used to generate downscaled precipitation results, and both agree in general trends. However, the precise levels of rainfall increases predicted by the two models vary substantially, and inferred changes were difficult to distinguish from natural variability given the relatively short simulation periods. While the differences between the two sets of current and future climate simulations are large enough to have potentially important consequences for the design of stormwater facilities, most are nonetheless not statistically significant.

Results of the hydrologic modeling on two urban watersheds in the central Puget Sound region affirm and extend both the broad trends and the substantial uncertainties evident in the precipitation simulations. For the two watersheds modeled, the simulations generally agree that peak discharges will increase, although the range of predicted change (from a slight decrease to a near-doubling, depending on the selected recurrence interval, watershed, and underlying GCM simulation) is much too large to provide a basis for engineering design. The comparative simulation results are most confounding for the smallest watershed areas, wherein even the net direction of change (i.e., a future increase or a future decrease) is in part dependent on the choice of GCM.

7 Conclusions

Our objectives in this paper were to characterize past and future trends in precipitation extremes across Washington State, with the ultimate goal of assessing the

impacts of climate change on its stormwater infrastructure. Despite some uncertainties amongst the results of our study, we offer the following conclusions in summary:

- Few statistically significant changes in extreme precipitation have been observed to date in the state's three major metropolitan areas, with the possible exception of the Puget Sound. Nonetheless, drainage infrastructure designed using mid-twentieth century rainfall records may be subject to a future rainfall regime that differs from current design standards.
- Projections from two regional climate model (RCM) simulations generally indicate increases in extreme rainfall magnitudes throughout the state over the next half-century, but their projections vary substantially by both model and region, and actual changes may be difficult to distinguish from natural variability.
- Hydrologic modeling of two urban creeks in central Puget Sound suggest overall increases in peak annual discharge over the next half-century, but only those projections resulting from one of the two RCM simulations are statistically significant. Magnitudes of projected changes vary widely, depending on the particular basin under consideration and the choice of the underlying global climate model.

Our assessment of future streamflows, and the magnitudes of peak discharges on which the design of stormwater infrastructure is based, suggests that concern over present design standards is warranted. However, because our analysis is based on only two GCMs, it is at most suggestive. For a more complete understanding of how precipitation extremes are likely to change in the future, the methods employed in the precipitation distribution analysis should be used to explore a larger sample of simulated climate data. Additional model simulations, based on a larger ensemble of GCMs and emission scenarios, will be required to develop a more robust set of conclusions and provide additional information for evaluating alternative stormwater-facility design standards.

Acknowledgements This study was conducted under the auspices of the University of Washington's Climate Impacts Group, with additional support provided by Seattle Public Utilities and Northwest Hydraulic Consultants (to DH), King County Water and Land Resources Division (to JB), and Stillwater Sciences (to DBB). We thank Rob Norheim for providing the maps and Lara Whitely Binder for reviewing an early draft of the paper. We would also like to acknowledge the encouragement and insights of Paul Fleming and Gary Schimek (City of Seattle) and the contributions of five anonymous reviewers, whose comments resulted in substantial improvements to the paper. This publication is part of the Washington Climate Change Impacts Assessment, funded by the 2007 Washington State Legislature through House Bill 1303. This publication is partially funded by the NOAA Regional Integrated Sciences and Assessments program and the NOAA Climate Dynamics and Experimental Prediction/Applied Research Centers program under NOAA Cooperative Agreement No. NA17RJ1232 to the Joint Institute for the Study of the Atmosphere and Ocean (JISAO). This is JISAO Contribution #1796.

References

Bicknell BR et al (1996) Hydrological Simulation Program—Fortran: User's manual for Release 11. US Environmental Protection Agency, Environmental Research Laboratory, Office of Research and Development, Athens, Georgia

Booth DB, Jackson CR (1997) Urbanization of aquatic systems—degradation thresholds, stormwater detention, and the limits of mitigation. J Am Water Resour Assoc 33(5):1077–1090

Choguill CL (1996) Ten steps to sustainable infrastructure. Habitat Int 20(3):389–404

Denault C, Millar RJ, Lence BJ (2002) Climate change and drainage infrastructure capacity in an urban catchment. Annual conference of the Canadian Society for Civil Engineering, Montreal, Quebec, Canada
Dinicola et al (1990) Characterization and simulation of rainfall-runoff relations for headwater basins in western King and Snohomish Counties, Washington. US Geological Survey Water-Resources Investigation Report 89-4052
Dinicola et al (2001) Validation of a numerical modeling method for simulating rainfall-runoff relations for headwater basins in western King and Snohomish Counties, Washington. US Geological Survey Water-Supply Paper 2495
Efron B (1979) Bootstrap methods: another look at the jackknife. Ann Stat 7(1):1–26
Fowler HJ, Kilsby CG (2003) A regional frequency analysis of United Kingdom extreme rainfall from 1961 to 2000. Int J Climatol 23:1313–1334
Gerstel WJ, Brunengo MJ, Lingley WS Jr, Logan RL, Shipman H, Walsh TJ (1997) Puget Sound bluffs: the where, why, and when of landslides following the 1996/97 storms. Wash Geol 25(1): 17–31
Groisman PY, Knight RW, Easterling DR, Karl TR, Hegerl GC, Razuvaev VN (2005) Trends in intense precipitation in the climate record. J Clim 18(9):1326–1350
Hamlet AF, Lee SY, Mickelson KEB, Elsner MM (2010) Effects of projected climate change on energy supply and demand in the Pacific Northwest and Washington State. Clim Change. doi:10.1007/s10584-010-9857-y
Hanson R (ed) (1984) Perspectives on urban infrastructure. Committee on National Urban Policy, National Research Council, Washington, DC. National Academies Press, 216 pp
Hosking JRM, Wallis JR (1997) Regional frequency analysis: an approach based on L-moments. Cambridge University Press, New York
Interagency Committee on Water Data (IACWD) (1982) Guidelines for determining flood flow frequency. Bulletin 17B (revised and corrected), Hydrology Subcommittee, Washington, DC
Intergovernmental Panel on Climate Change (IPCC) (2007a) Climate change 2007: the physical science basis. Geneva, Switzerland
Intergovernmental Panel on Climate Change (IPCC) (2007b) Climate change 2007: synthesis report. contribution of working groups I, II and III to the fourth assessment report of the Intergovernmental Panel on Climate Change [core writing team Pachauri RK, Reisinger A eds.] Geneva, Switzerland
Karl TR, Knight RW (1998) Secular trends of precipitation amount, frequency, and intensity in the United States. Bull Am Meteorol Soc 79(2):231–241
King County (1985) Juanita Creek basin plan. King County Department of Public Works, Surface Water Management Division, Seattle, Washington
Kirschen P, Ruth M, Anderson M, Lakshmanan TR (2004) Infrastructure systems, services and climate change: Integrated impacts and response strategies for the Boston metropolitan area. Tufts University: Climate's Long-term impacts on metro Boston (CLIMB). USEPA Grant Number R.827450-01, Final report. http://www.aia.org/SiteObjects/files/CLIMB%20Executive%20Summary.pdf. Accessed 6 Dec 2008
Konrad CP, Booth DB (2002) Hydrologic trends associated with urban development for selected streams in the Puget Sound basin, western Washington. US Geological Survey Water Resources Investigations Report No. 4040
Kunkel KE, Andsager K, Easterling DR (1999) Long-term trends in extreme precipitation events over the conterminous United States and Canada. J Clim 12:2515–2527
Kunkel KE, Easterling DR, Redmond K, Hubbard K (2003) Temporal variations of extreme precipitation events in the United States: 1895–2000. Geophys Res Lett 30(17):1900
Larsen P, Goldsmith S (2007) How much might climate change add to future costs for public infrastructure? Institute of Social and Economic Research, University of Alaska Anchorage. UA Research Summary No. 8
Leopold LB (1968) Hydrology for urban land planning—a guidebook on the hydrologic effects of urban land use. Geol Surv Circ 554, 18 pp
Leung LR, Kuo YH, Tribbia J (2006) Research needs and directions of regional climate modeling using WRF and CCSM. Bull Am Meteorol Soc 87:1747–1751
Lettenmaier DP (1976) Detection of trends in water quality data with dependent observations. Water Resour Res 12(5):1037–1046
Lettenmaier DP, Wallis JR, Wood EF (1987) Effect of regional heterogeneity on flood frequency estimation. Water Resourc Res 23(2):313–324

Madsen T, Figdor E (2007) When it rains, it pours: global warming and the rising frequency of extreme precipitation in the United States. Report prepared by Environment America Research and Policy Center, Boston

Mote P, Salathé E, Peacock C (2005) Scenarios of future climate for the Pacific Northwest. Report prepared by the Climate Impacts Group, Center for Science in the Earth System, Joint Institute for the Study of the Atmosphere and Oceans, University of Washington, Seattle. http://cses.washington.edu/db/pdf/kc05scenarios462.pdf

Payne JT et al (2004) Mitigating the effects of climate change on the water resources of the Columbia River Basin. Clim Change 62(1–3):233–256

Pryor SC, Howe JA, Kunkel KE (2009) How spatially coherent and statistically robust are temporal changes in extreme precipitation in the contiguous USA? Int J Climatol 29:31–45

Richter BD, Baumgartner JV, Powell J, Braun DP (1996) A method for assessing hydrologic alteration within ecosystems. Conserv Biol 10:1163–1174

Salathé EP (2005) Downscaling simulations of future global climate with application to hydrologic modeling. Int J Climatol 25(4):419–436

Salathé EP, Steed R, Mass CF, Zahn P (2008) A high-resolution climate model for the U.S. Pacific Northwest: Mesoscale feedbacks and local responses to climate change. J Clim 21:5708–5726

Salathé EP, Leung LR, Qian Y, Zhang Y (2010) Regional climate model projections for the State of Washington. Clim Change. doi:10.1007/s10584-010-9849-y

Shaw H, Reisinger A, Larsen H, Stumbles C (2005) Incorporating climate change into stormwater design—why and how? South Pacific Conference on Stormwater and Aquatic Resource Protection, Ministry for the Environment, Auckland, New Zealand

Trenberth K, Dai A, Rasmussen RM, Parsons DB (2003) The changing character of precipitation. Bull Am Meteorol Soc 84(9):1205–1217

Urbonas BR, Roesner LA (1993) Hydrologic design for urban drainage and flood control. In: Maidment DR (ed) Handbook of hydrology. McGraw-Hill, New York

Vano JA, Voisin N, Cuo L, Hamlet AF, Elsner MM, Palmer RN, Polebitski A, Lettenmaier DP (2010a) Climate change impacts on water management in the Puget Sound region,Washington State, USA. Clim Change. doi:10.1007/s10584-010-9846-1

Vano JA, Voisin N, Scott M, Stockle CO, Hamlet AF, Mickelson KEB, Elsner MM, Lettenmaier DP (2010b) Climate change impacts on water management and irrigated agriculture in the Yakima River Basin, Washington, USA. Clim Change. doi:10.1007/s10584-010-9856-z

Wallis JR, Schaefer MG, Barker BL, Taylor GH (2007) Regional precipitation-frequency analysis and spatial mapping for 24-hour and 2-day durations for Washington State. Hydrol Earth Syst Sci 11(1):415–442

Washington State Department of Transportation (WSDOT) (2008) Storm-related closures of I-5 and I-90: Freight Transportation Economic Impact Assessment Report. Washington State Department of Transportation WA-RD 708.1

Waters D, Watt WE, Marsalek J, Anderson BC (2003) Adaptation of a storm drainage system to accommodate increased rainfall resulting from climate change. J Environ Plan Manag 46(5): 755–770

Watt WE, Waters D, Mclean R (2003) Climate variability and urban stormwater infrastructure in Canada: Context and case studies. Toronto-Niagara Region Study Report and Working Paper Series, Meteorological Service of Canada, Waterloo, Ontario, Canada

Wilks DS (2006) Statistical methods in the atmospheric sciences, Second Edition. Academic Press

Wood AW, Maurer EP, Kumar A, Lettenmaier DP (2002) Long-range experimental hydrologic forecasting for the eastern United States. J Geophys Res 107(D20):4429